Progress In Electromagnetics Research C, Vol. 24, 147–159, 2011

A COMPACT DOUBLE-BALANCED STAR MIXER WITH NOVEL DUAL 180° HYBRID

Y.-A. Lai [1], C.-N. Chen [1], C.-C. Su [1], S.-H. Hung [1], C.-L. Wu [1, 2], and Y.-H. Wang [1, 3, *]

[1]Institute of Microelectronics, Department of Electrical Engineering, National Cheng-Kung University, No. 1 University Road, Tainan 70101, Taiwan

[2]Transcom Inc., Tainan, Taiwan

[3]National Applied Research Laboratories, Taipei 106, Taiwan

Abstract—A compact double-balanced monolithic star mixer for Ka-band applications using 0.25 µm GaAs pHEMT process is presented. With multi-coupled lines technology, the proposed dual 180° hybrid is produced and applied to a star mixer successfully. The proposed hybrid adopts the power divider and two types of multi-coupled lines to improve the return loss and isolation at the balance outputs of a traditional dual Marchand balun. Output ports are allowed to locate arbitrarily, eliminating a complex layout while the dual 180° hybrid is applied to double balanced star mixers. As the measurement results show, the proposed mixer achieves an operation bandwidth of 27 to 36 GHz with the best conversion loss of 6.3 dB at 28 GHz. In addition, the chip dimension can be manufactured as small as 0.81 mm^2.

1. INTRODUCTION

Recently, the burgeoning techniques for multipoint, radars, and satellite communication systems have been promoted in millimeter-wave. In these systems, the function of a mixer is to convert signals from high frequency to a low frequency or vice versa [1]. Previous mixer designs often utilize balanced configurations. Balanced-type mixers are advantageous for communication systems that use millimeter-wave applications because of low conversion loss and good port-to-port isolation in broad bandwidth [2].

Received 9 August 2011, Accepted 1 September 2011, Scheduled 22 September 2011

* Corresponding author: Yeong-Her Wang (yhw@ee.ncku.edu.tw).

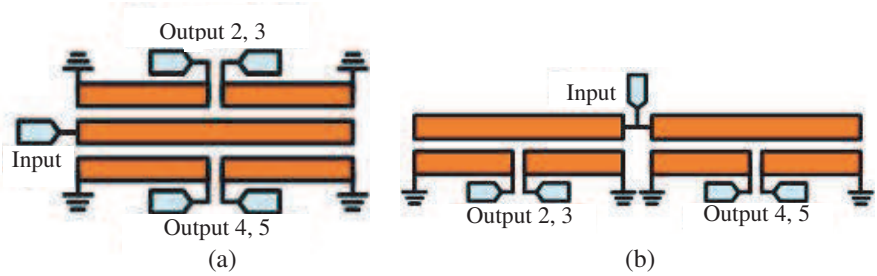

Figure 1. Conventional dual Marchand balun structures in a mixer.

Double-balanced star mixers are often used among balanced mixers. Due to the dual anti-phase relationships of local oscillator (LO) and radio frequency (RF), the intermediate frequency (IF) port presents a virtual ground to both LO and RF signals, isolating the IF port from the other ports. However, traditional star mixers need two large crossover dual Marchand balun structures, as they increase inflexibility in design and circuit dimension.

Therefore, many new topologies for star mixers have been proposed to reduce dual Marchand balun structures. These topologies utilize the novel planar Marchand balun, compensated capacitors, and coplanar waveguide structure to achieve a compact purpose [3–6]. Previous mixers were based on the dual Marchand balun structure, which may have complex IF extraction circuit and large chip dimensions [7–12], as shown in Fig. 1. These methods might cause layout complications and present difficulties in integrating the mixer into a low-cost and compact system. Furthermore, conventional dual Marchand baluns cannot achieve perfect matching at balanced ports, resulting in degraded mixer performance. Therefore, a compact and flexible dual 180° hybrid needs further investigation, especially for well-matching and effective circuits.

In this paper, a novel configuration of a double-balanced star mixer with a new dual 180° hybrid is presented. The proposed double-balanced star mixer can ignore RF/LO balun crossover issue and reduce the LO signal power requirement as well.

2. DESIGN OF THE PROPOSED STAR MIXER CONFIGURATION

2.1. Dual 180° Hybrid

The proposed hybrid consists of a power divider, open stubs, and short stubs as shown in Fig. 2. The power divider is used to split the equal

in-phase signal power, while the open/short stubs with three-conductor coupled lines are employed as phase shifters to produce the anti-phase outputs.

The open/short stubs phase shifters can be simplified as two-conductor coupled lines for analysis as shown in Fig. 3(a) and can be referred to as the four-port network, then simplified as the two-port network cases as shown in Figs. 3(b) and (c) [13]. The four port network with S-parameters can be simply expressed as follows:

$$\begin{bmatrix} b_1 \\ b_2 \\ b_3 \\ b_4 \end{bmatrix}_{\substack{\text{Four-port} \\ \text{coupler}}} = 1/\sqrt{2} \begin{bmatrix} 0 & 0 & -j & 1 \\ 0 & 0 & 1 & -j \\ -j & 1 & 0 & 0 \\ 1 & -j & 0 & 0 \end{bmatrix} \begin{bmatrix} a_1 \\ a_2 \\ a_3 \\ a_4 \end{bmatrix} \tag{1}$$

Assuming ports 3 and 4 are terminated in an open circuit, then $a_3 = b_3$ and $a_4 = b_4$. If ports 3 and 4 are terminated in a short circuit, then $a_3 = -b_3$ and $a_4 = -b_4$. The results present two-port networks with S-matrix given by Equation (2):

$$[S]_{\substack{\text{open} \\ \text{stub}}} = \begin{bmatrix} 0 & -j \\ -j & 0 \end{bmatrix} \quad \& \quad [S]_{\substack{\text{short} \\ \text{stub}}} = \begin{bmatrix} 0 & j \\ j & 0 \end{bmatrix} \tag{2}$$

The open stub circuit with a $-90°$ phase shift and the short stub circuit with a $90°$ phase shift can be obtained, resulting in a $180°$ differential phase. The analysis of the proposed dual $180°$ hybrid by the five-port network is shown in Fig. 2. Based on the multi-coupled line analysis, the three-conductor coupled lines can be approximated as two pairs of two-conductor coupled lines with no mutual coupling [14].

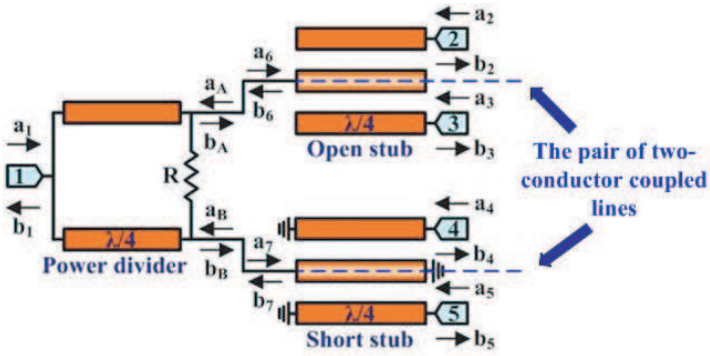

Figure 2. The proposed dual $180°$ hybrid can be analyzed through the five-port network.

Figure 3. (a) The four-port coupled line. (b) Two-port open stub circuit. (c) Two-port short stub circuit.

Thus, the S-parameters of the open/short stubs can be derived from the Equation (2), and results in two parts with $+/-90°$ phase differences. The three-port networks are expressed as follows:

$$\begin{cases} b_2 = b_3 = -\frac{j}{\sqrt{2}} a_6 \\ b_6 = -\frac{j}{\sqrt{2}}(a_2 + a_3) \end{cases}_{\substack{\text{Three-port} \\ \text{open stub}}} \& \begin{cases} b_4 = b_5 = \frac{j}{\sqrt{2}} a_7 \\ b_7 = \frac{j}{\sqrt{2}}(a_4 + a_5) \end{cases}_{\substack{\text{Three-port} \\ \text{short stub}}} \tag{3}$$

The power divider can be referred to as the three-port network as follows:

$$\begin{cases} b_1 = \dfrac{-j}{\sqrt{2}}(a_A + a_B) \\ b_A = \dfrac{-j}{\sqrt{2}} a_1 \\ b_B = \dfrac{-j}{\sqrt{2}} a_1 \end{cases}_{\text{Power divider}} \tag{4}$$

When the output port of the power divider and the input port of the open/short stubs are connected, the following can be obtained as: $b_A = a_6$, $a_A = b_6$, $b_B = a_7$, and $a_B = b_7$. Accordingly, a five-port network is given by:

$$\begin{bmatrix} b_1 \\ b_2 \\ b_3 \\ b_4 \\ b_5 \end{bmatrix}_{\substack{5 \text{ port} \\ \text{network}}} = 1/2 \begin{bmatrix} 0 & -1 & -1 & 1 & 1 \\ -1 & 0 & 1 & 0 & 0 \\ -1 & 1 & 0 & 0 & 0 \\ 1 & 0 & 0 & 0 & 1 \\ 1 & 0 & 0 & 1 & 0 \end{bmatrix} \begin{bmatrix} a_1 \\ a_2 \\ a_3 \\ a_4 \\ a_5 \end{bmatrix} \tag{5}$$

Finally, in combining the power divider and open/short stubs, the four output ports with the dual anti-phase and equal power splitting characteristics are obtained. In addition, the output ports are perfectly matched and isolated. Therefore, the proposed hybrid can be identified as the five-port network of an ideal dual 180° hybrid. Compared with the dual Marchand balun, the dual 180° hybrid structure can improve the return loss and port-to-port isolation. Accordingly, the proposed hybrid for the star mixer can meet the required performance.

In order to compare the proposed dual 180° hybrid with the conventional topology as shown in Fig. 1(a), the proposed hybrid and conventional dual Marchand balun were operated at 2.4 GHz using planar coupled-line, designed and implemented on an FR-4 printed

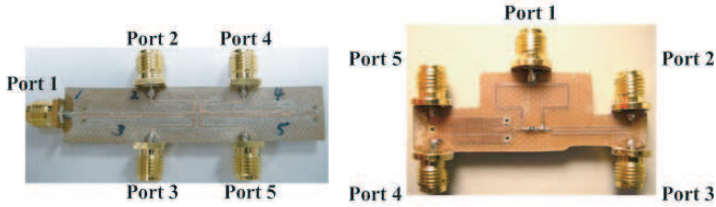

(a) (b)

Figure 4. Photograph of the fabricated. (a) Conventional dual Marchand balun. (b) Proposed dual 180° hybrid.

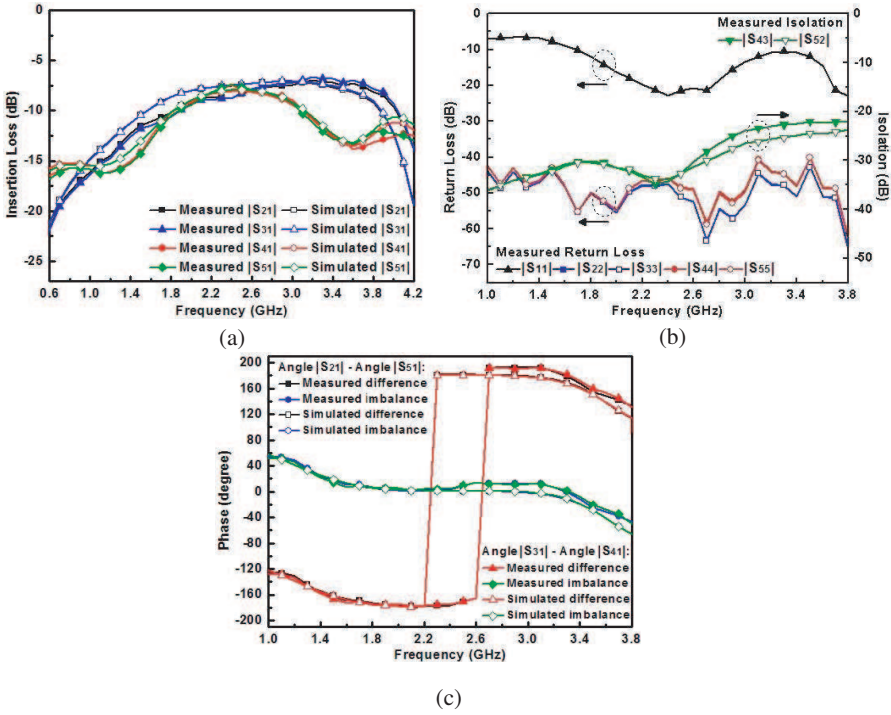

(a) (b) (c)

Figure 5. Simulated and measured S-parameters of the proposed dual-balun at the RF range of 1–3.8 GHz. (a) Insertion loss. (b) Return loss. (c) Phase.

circuit board (PCB) as shown in Fig. 4. The FR-4 PCB with a dielectric constant of 4.4 and thickness of 0.8 mm was employed. In the proposed hybrid, the transmission line values of the power divider length and width were 19.3 and 0.6 mm, respectively. The value of resistor R was set to 150 ohm (Fig. 2.), which was different from the value of isolation resistance at 100 ohm in traditional power dividers. Inasmuch as the properties of open/short stubs were different, the higher resistance was used to match the impedance between the power divider and open/short stubs. Insertion losses could then be reduced, but the isolation between the balanced ports would remain the same. The $\lambda/4$ coupled-line values for the length, width, and spacing of the open stub were 15.8, 0.3, and 0.4 mm, respectively, while those for the short stub were 14.9, 1.6, and 0.1 mm, respectively The $\lambda/4$ coupled-line values of the length, width, and spacing of the dual Marchand balun were 21, 0.4, and 0.1 mm, respectively. The coupled lines spacing is limited by the fabrication process.

Figure 5 shows the simulated and measured S-parameters of the proposed dual balun at the RF range of 1 to 3.8 GHz. The results of insertion losses $|S_{21}|$, $|S_{31}|$, $|S_{41}|$, and $|S_{51}|$, as well as the output power characteristics of the dual 180° hybrid, are shown in Fig. 5(a). The measured insertion losses were 7.2–9.4 dB from 2 to 3 GHz, which is similar to simulated results and it also indicates that the proposed hybrid can successfully split an incoming signal into four equivalent amplitude outputs with wide bandwidths.

The measured results of the return loss and isolation as a function of frequencies are shown in Fig. 5(b). From 1 to 3.8 GHz, the measured return loss of $|S_{22}|$, $|S_{33}|$, $|S_{44}|$, and $|S_{55}|$were also lower than −40.1 dB; while the measured return loss of $|S_{11}|$was lower 22 dB at 2.4 GHz. Similar to the results from analysis, the designed circuit well matched all the ports. At 2–2.8 GHz, the measured isolation of $|S_{43}|$and $|S_{52}|$was lower than −26.4 dB. Similar to the results from analysis, the designed circuit well matched all the ports. Good isolation was also observed for the balanced ports, indicating that the proposed hybrid can meet the required performance of the balanced circuit.

The measured and simulated results of the relative phase difference and imbalance between the balanced ports are shown in Fig. 5(c). The phase difference between ports 2 and 5 was 176.3° ; between ports 3 and 4, it was 175.5° at the center frequency of 2.4 GHz. Phase imbalances were less than 6° within the bandwidth at 1.9–2.4 GHz, indicating good anti-phase balance.

Table 1 summarizes the architectures of the proposed hybrid and the conventional dual Marchand balun. This dual 180° hybrid delivers flexible configuration and efficient performance.

Table 1. Comparison of dual marchand balun with the proposed hybrid.

Architecture (Frequency @ 2.4 GHz)	Conventional type	This work
Insertion Loss (dB)	$6.9 \sim 7.1$	$7.4 \sim 8.8$
Phase Difference (degree)	181.2/180.5	176.3/175.5
Isolation* (dB)	16.1/15.9	34.3/33.8
Input Return Loss (dB)	9.1	22.9
Output Return Loss (dB)	$2.1 \sim 2.3$	$45.7 \sim 47.5$
Output ports at the same side	no	yes

$*$ Between the balanced ports

2.2. Star Mixer Configuration

The traditional star mixer can be simplified by using dual 180° hybrid as shown in Fig. 6. The quarter wavelength of transmission-line in power divider usually occupies most of the chip area. To reduce the size of the power divider, the quarter wavelength of the transmission line is replaced with a π-network, consisting of a short high-impedance line with a shunt capacitor at the value of $C = 0.1$ pF at each port. The RF/LO signals are divided among balanced ports with out-phase signals by two dual 180° hybrids and transferred to the gates of four diodes. The mixer prevents the RF/LO balun crossover structure in the two dual Marchand baluns and easily extracts the IF signals from the common node. In the IF port, the low-pass filter (LPF) was realized by a transmission line and a capacitor. Using a transmission line instead of a quarter-wave open circuit can minimize the number of circuit elements. Thus, the isolation and the chip size can be further improved. To decrease the chip area of the matching circuits, 90° hybrid could be designed to provide broadband matching to the diodes directly instead of matching to 50 Ω.

3. MIXER IMPLEMENTATION AND RESULTS

This mixer was fabricated using a low-noise gallium arsenide pseudomorphic high electron mobility transistor (GaAs PHEMT) process on a 78 µm thick GaAs substrate from Transcom Inc. A wide-head 0.25 µm T-shaped gate, air bridges, via-hole etching, and back-side processing were used during device fabrication. In this

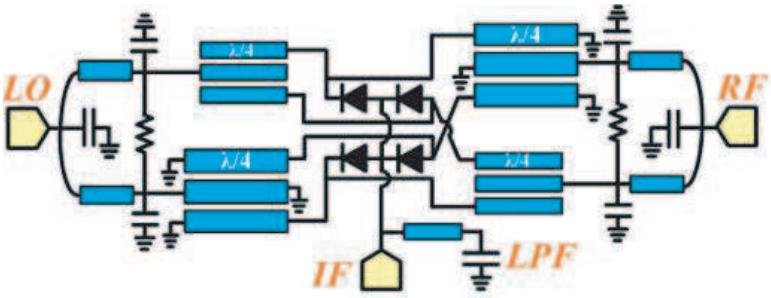

Figure 6. Configuration of the proposed mixer with the proposed novel dual 180° hybrid.

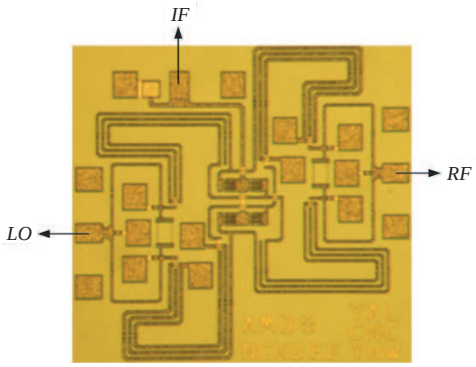

Figure 7. A photograph of the fabricated star mixer. The chip dimension including the contact pads is $0.93 \times 0.87\,\text{mm}^2$.

case, 4 Schottky diodes were used to realize the proposed dBm. To achieve appropriate impedance matching between the dual balun and the Schottky diode, a 8-finger Schottky diode's model with a 100 μm gate width was optimized to ensure minimum conversion loss. The $\lambda/4$ coupled-line value for the length of the power divider was 425 μm, while 975 and 930 μm for the short stub and open stub, respectively. The chip dimension of the proposed dual balun is $0.68 \times 0.38\,\text{mm}^2$. A photograph of the fabricated circuit is shown in Fig. 7. The chip size of the fabricated mixers is $0.93 \times 0.87\,\text{mm}^2$.

To dimension the transmission lines of proposed dual balun, lump-element model was used. Electronic design automation softwares, including advanced design system (ADS) and microwave office (MWO), were utilized to synthesize the hybrid in the initial designs. A full-wave EM simulator, ADS Momentum, was used after the initial design to

predict the performance more precisely. ADS Momentum was used to calculate the S-parameters of the passive structures for circuit simulations and then to optimize the geometry of the baluns to reduce insertion loss and phase imbalance, and thus reduce the conversion loss of DBM.

The fabricated mixer was attached on carrier plates for testing. The measurements of the signals were provided by a coplanar GSG on-wafer probes measurement system based on the Agilent E4446A spectrum analyzer, which was calibrated using an E44198 power meter. The losses of probes and cables were calibrated using the two ports of PNA E8364A network analyzer.

Figure 8 shows the measured and simulated conversion loss versus the LO input power of the mixer at the LO frequency of 27 GHz with −15 dBm of the RF power and the IF fixed at 1 GHz. A significant mixing effect at an LO drive level of 9 dBm can be seen. The best conversion loss is 6.8 dB at 14 dBm LO power level. Good impedance matching between the Schottky diodes and hybrid's output ports indicates that the Schottky diodes and hybrid's output ports can improve the conversion loss with lower LO driving power.

Due to the drive of 4 diodes in the nonlinear characteristics of the star mixer, the required LO power is relative high. In the mixer measurement, LO drive power level was set to 14 dBm and RF power level was set to approximately −15 dBm to achieve optimum performance based on the Fig. 8. Fig. 9 shows the measured and simulated conversion loss of the mixer with an RF frequency of 26–38 GHz. The measured conversion loss of the mixer is between 6.3 and 13.6 dB from 27 to 36 GHz, with the IF fixed at 1 GHz. The conversion

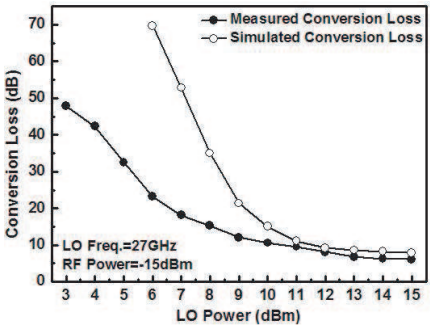

Figure 8. Conversion loss versus the LO input power at the LO frequency of 27 GHz.

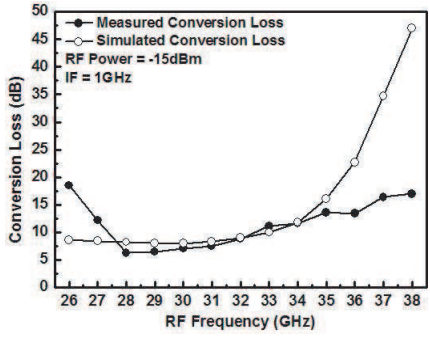

Figure 9. Conversion loss versus RF frequency when the IF is fixed at 1 GHz.

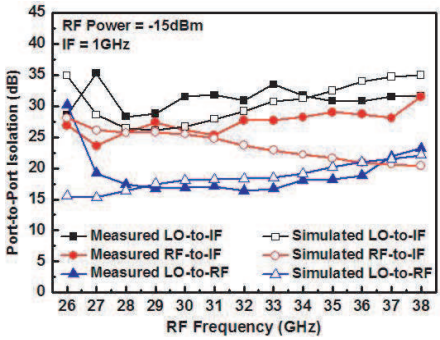

Figure 10. Port-to-port isolation at the 14 dBm LO power level and 1 GHz IF frequency.

loss is better than 9 dB from 28 to 32 GHz and 13.6 dB from 33 to 36 GHz.

Figure 10 shows the measured and simulated results of LO-to-RF, LO-to-IF, and RF-to-IF isolations as functions of RF frequency from 26 to 38 GHz. The measured LO-to-IF and RF-to-IF isolation were better than 23.6 dB from 26 to 38 GHz. Thus, LPF could provide superior isolation between IF and LO/RF ports. The LO-to-RF isolation of mixer is then limited to the inherent condition of the proposed structures, consequently resulting in 16.4 to 23.2 dB from 27 to 38 GHz. The mixer performs efficiently and proves that the new hybrid is workable.

Figure 11 shows the conversion loss against the RF input power with the RF fixed at 28 GHz and the IF fixed at 1 GHz. The measured result of mixer exhibits low conversion loss at 6.3 dB, while the measured 1 dB compression point is 11 dBm.

Figure 12 shows the response of conversion loss as a function of the IF bandwidth with LO fixed at 27 GHz. The measured conversion loss is between 6.3 and 12.6 dB from DC to 6 GHz IF frequencies. Thus, the IF extraction circuit helps increase the IF bandwidth of a star mixer.

Deviations between simulated and measured results are observed. The simulated conversion loss is even higher than that of measured. The discrepancy may mainly attribute to the pHEMT gate reflow process to deviate the Schottky diode nonlinear large signal model. High frequency parasitics of the passive elements and transmission lines may also cause the shift of the impedance matching. This will make the influence on the mixing performance of the DBM.

The performances of the double-balanced mixers compared with those exhibited in previous works are summarized in Table 2 [5–10, 15].

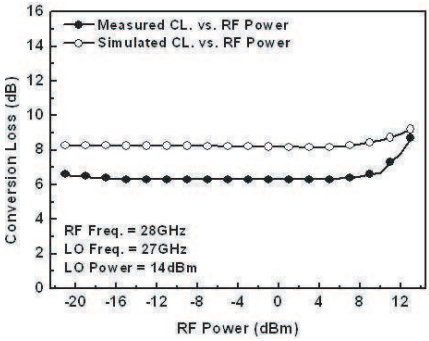

Figure 11. Measured and simulated conversion loss versus the RF input power at the LO input power of 14 dBm.

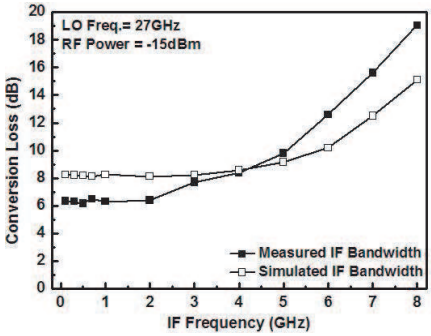

Figure 12. Conversion loss of the proposed mixer as a function of IF bandwidth when the LO frequency is at −15 dBm RF power level.

Table 2. Comparison of the reported pHEMT millimeter-wave double-balanced mixers.

	[2]	[5]	[6]	[7]	[8]	[9]	[10]	[15]	This Work
Technology	0.25 µm	0.15 µm	0.1 µm	0.25 µm	0.15 µm	0.15 µm	0.15 µm	---	0.25 µm
RF frequency (GHz)	28–36	52–68	50–75	29–40	16–44	25–50	26–38	30–45	27–36
LO power (dBm)	12	12	13	15	15	13	12	4	14
LO-to-IF isolation (dB)	>24	>18	N/A	>23.4	>27	>30	>29	N/A	>26.1
P1dB (dBm)	N/A	7.7	3	15	14	5	13	1.4	11
Conversion loss (dB)	11.9–15.7	8.6–12. 5	13–18	10.3–14.7	11–14	7–12	5.4–10.7	10–14	6.3–13.6
Chip size (mm^2)	2.89	0.4	2.25	1.4	0.64	1	2.5	4	0.81

In this paper, the proposed hybrid was easy for designing output port in any directions, and eliminated RF/LO balun crossover structure in the star mixer. Therefore, the proposed technique is more convenient in circuit layout with improved mixer's performance as compared with conventional DBMs. The chip area, including pads, is as small as 0.81 mm^2, which is relatively compact among published pHEMT mixers. Moreover, the proposed hybrid can be used to improve the conversion loss and port-to-port isolations of the star mixer.

4. CONCLUSION

A compact and broadband star mixer with a new dual 180° hybrid has been presented. The novel dual 180° hybrid can easily transfer the impedance of the input terminal to the terminal of diodes, and eliminates the RF/LO balun crossover structure in the double-balanced star mixer. This star mixer has well matching at the balanced ports, reducing LO power drive requirements and improves conversion loss. Furthermore, this mixer achieved low conversion loss of 6.3 dB and a wide operation bandwidth from 27 to 36 GHz. The LO-to-IF and RF-to-IF isolations are higher than 28.3 and 23.6 dB from 26 to 38 GHz, respectively. Compared with previous studies, the proposed configuration provides a novel hybrid in designing a monolithic microwave integrated circuit mixer with a compact size, which is attractive for RF front-end applications.

ACKNOWLEDGMENT

This work was supported in part by the National Science Council of Taiwan under contracts NSC NSC95-2221-E-006-428-MY3, 982C12, 98IC05 and the Foundation of Chen, Jieh-Chen Scholarship of Tainan, Taiwan.

REFERENCES

1. Mondal, J., J. Geddes, J. Detry, and D. Carlson, "Ka-band MMIC receiver with ion-implanted technology for high-volume and low-cost application," *IEEE Microw. Guided Wave Lett.*, Vol. 1, No. 10, 278–281, Oct. 1991.
2. Lin, C. H., J. C. Chiu, C. M. Lin, Y. A. Lai, and Y. H. Wang, "A variable conversion gain star mixer for Ka-band applications," *IEEE Microw. Wireless Compon. Lett.*, Vol. 17, No. 11, 802–804, Nov. 2007.
3. Basu, S. and S. A. Maas, "Design and performance of a planar star mixer," *IEEE Trans. on Microw. Theory Tech.*, Vol. 41, No. 11, 2028–2030, Nov. 1993.
4. Kim, S. S., J. H. Lee, and K. W. Yeom, "A novel planar dual balun for doubly balanced star mixer," *IEEE Microw. Wireless Compon. Lett.*, Vol. 14, No. 9, 440–442, Sep. 2004.
5. Yang, T. Y., W. R. Lien, C. C. Yang, and H. K. Chiou, "A compact V-band star mixer using compensated overlay capacitors

in dual baluns," *IEEE Microw. Wireless Compon. Lett.*, Vol. 17, No. 7, 537–539, Jul. 2007.

6. Yeom, K. W. and D. H. Ko, "A novel 60-GHz monolithic star mixer using gate-drain-connected pHEMT diodes," *IEEE Trans. Microw. Theory Tech.*, Vol. 53, No. 7, 2435–2440, Jul. 2005.
7. Lai, Y. A., S. H. Hung, C. N. Chen, and Y. H. Wang, "A millimeter-wave monolithic star mixer with simple IF extraction circuit," *Journal of Electromagnetic Waves and Applications*, Vol. 23, No. 17–18, 2433–2440, 2009.
8. Lin, C. M., H. K. Lin, C. F. Lin, Y. A. Lai, C. H. Lin, and Y. H. Wang, "A 16-44 GHz compact doubly balanced monolithic ring mixer," *IEEE Microw. Wireless Compon. Lett.*, Vol. 18, No. 9, 620–622, Sep. 2008.
9. Kuo, C. C., C. L. Kuo, C. J. Kuo, S. A. Maas, and H. Wang, "Novel miniature and broadband millimeter-wave monolithic star mixers," *IEEE Trans. Microw. Theory Tech.*, Vol. 56, No. 4, 793–802, Apr. 2008.
10. Lin, C. H., C. M. Lin, Y. A. Lai, and Y. H. Wang, "A 26-38 GHz monolithic doubly balanced mixer," *IEEE Microw. Wireless Compon. Lett.*, Vol. 18, No. 9, 623–625, Sep. 2008.
11. Chiou, H. K. and J. Y. Lin, "Symmetric offset stack balun in standard 0.13-μm CMOS technology for three broadband and low-loss balanced passive mixer designs," *IEEE Trans. Microw. Theory Tech.*, Vol. 59, No. 6, 1529–1538, Jun. 2011.
12. Mongia, R., I. Bahl, and P. Bhartia, *RF and Microwave Coupled-Line Circuits*, Artech House, Norwood, MA, 1999.
13. Risueño, G. L. and J. I. Alonso, "Simulation of interdigitated structures using two-coupled line models," *Microwave Journal*, Vol. 43, No. 6, 70–82, Jun. 2000.
14. Ahn, H. R., K. Lee, and N. H. Myung, "General design equations of N-way arbitrary power dividers," *IEEE MTT-S Int. Microwave Symp. Dig.*, Vol. 1, 65–68, Jun. 2004.
15. Yu, M., R. H. Walden, A. E. Schmitz, and M. Lui, "Ka/Q-band doubly balanced MMIC mixers with low LO power," *IEEE Microw. Guided Wave Lett.*, Vol. 10, No. 10, 424–426, Oct. 2000.